P11 Observations of Appalachian Fronts during Two NSF Educational Deployments

Brian J. Billings*
Department of Earth Sciences, Millersville University, Millersville, PA

1. BACKGROUND

1.1 *NSF Educational Deployment Program*

Hands-on, experiental learning is widely accepted to have great value to students of meteorology. Because of this, part of NSF's Lower Atmospheric Observing Facilities remains reserved for deployments to college campuses. Participating organizations are the Center for Severe Weather Research, University of Wyoming, and National Center for Atmospheric Research's Earth Observing Laboratory, the latter also managing the proposal process and website at `www.eol.ucar.edu/educational-deployments` (refer to this site for project acronyms). Table 1 lists the requestable facilities from each organization.

Center for Severe Weather Research
Doppler on Wheels (HERO, C-BREESE, etc.)
Weather Pods (BASS)
Earth Observing Laboratory
Mobile Integrated Sounding System (BaSE CaMP)
Integrated Surface Flux System (CWEX, CABL)
University of Wyoming (with special consideration)
King Air (START)

Table 1: Organizations and requestable facilities in the NSF educational deployment pool

EOL's Mobile Integrated Sounding system was first deployed in EDUCT at the University of Virginia and later in two deployments at Saint Cloud State University called BaSE CaMP. There have also been deployments of EOL's Integrated Surface Flux System, such as ARTSE during the recent total solar eclipse. However, the most requests have been for the CSWR's Doppler on Wheels (DOWs), though the system's weather pods can also be requested separately. A review of the use of DOWs in educational requests is given by Milrad and Herbster (2017). While deployments are usually limited to a funding total of $25k, in special cases the University of Wyoming King Air has been deployed through this program. The first example was START at Embry-Riddle in Prescott. Figure 1 shows students working with a DOW and the King Air.

While these awards are smaller than many grants for science and education, there is still a great deal of value that can be gained from them with effective use. This is true of both the student engagement and public outreach components and the collection of quality datasets for later research purposes. An illustration of this from the two BaSE CaMP projects is given in an upcoming paper by Billings et al. (2018).

*Corresponding author address: Brian Billings, Department of Earth Sciences, Millersville University, PO Box 1002, Millersville, PA; e-mail: brian.billings@millersville.edu

FIG. 1: Millersville university students participate in the deployment of a Doppler on Wheels (left) and the Wyoming King Air (right).

1.2 *Millersville University Requests*

In an eighteen month period Millersville University was the host institution of two educational deployments of two different instrument platforms. Millersville is located in southeastern Pennsylvania, both 50 mi east and 25 mi south of the Appalachian mountains due to being located near a change in orientation of the range. This unique topographic setting was an important point in both project proposals.

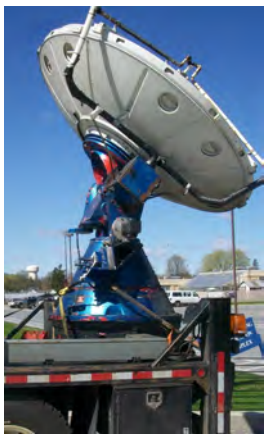

FIG. 2: The Doppler on Wheels operating during MEDOW IOP 1. The Millersville water tower is visible to the right above the tree line.

The first project in March-April 2016 was Millersville University Educational Doppler on Wheels (MEDOW) which included a student on the educational deployment proposal for the first time. After training sessions for the students in Radar Meteorology and visits to two public outreach events, the DOW was sent on three intensive observing periods. While work with the radar was mostly

reserved for Radar Meteorology, one IOP was based on a calibration exercise for Physical Meteorology students who had just learned the radar equation.The target was the Millersville water tower seen behind the antennae in Fig. 2. The other two IOP's were during frontal passages and both resulted in observations of interactions with the Appalachian terrain which will be examined shortly.

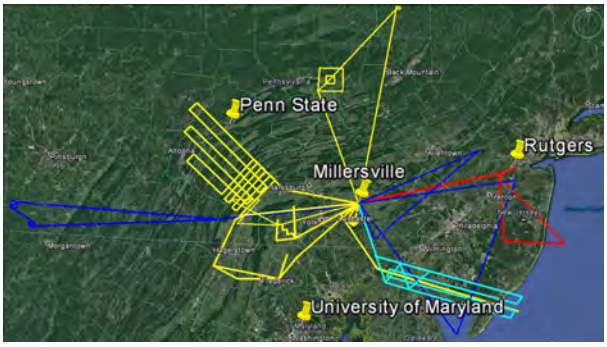

FIG. 3: Participating universitiy locations and proposed flight tracks for SEAR-MAR.

The second deployment in November 2017 was of the King Air and called Student Experience in Airborne Research in the Mid-Atlantic Region (SEAR-MAR), which was even larger in scale than START due to including four different universities. Their locations and the proposed flight tracks are shown in Fig. 3. Some of the missions were planned with heavy student involvement. Examples include methane sampling flights designed by students in a graduate class at Penn State, a cold air damming flight with remote Windsonde launches that were planned and executed by a Millersville student research group, and a cold air pool flight that was independently designed and coordinated by a Millersville student. Other missions were designed by faculty members based on predefined scientific objectives. These included the passage of a cold front over the Appalachians and mountain waves in the post-frontal environment, both of which will be further examined in this presentation.

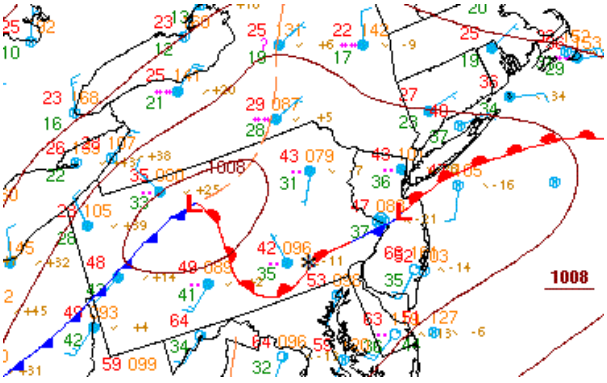

FIG. 4: WPC surface analysis for 15 UTC 04 April 2016. Millersville is shown by the asterisk.

2. MEDOW IOP 2 - COLD FRONT

A key goal of MEDOW was to show the value of an X-band radar in an area of poor NEXRAD coverage. The precipitation event that was targeted for this purpose was a cold frontal passage on 4 April 2016. Figure 4 shows that this front was not replacing a much warmer air mass due to apparent in-situ cold-air damming over the study area. However, the post-frontal air was cold enough to sink down the lee slopes of the mountains as seen by the clearing in Fig. 5. This clearing propogates eastward along the mountains as the front advances forward, while a thin line of cloud at the leading edge of this clearing appears thicker than that over the rest of the area.

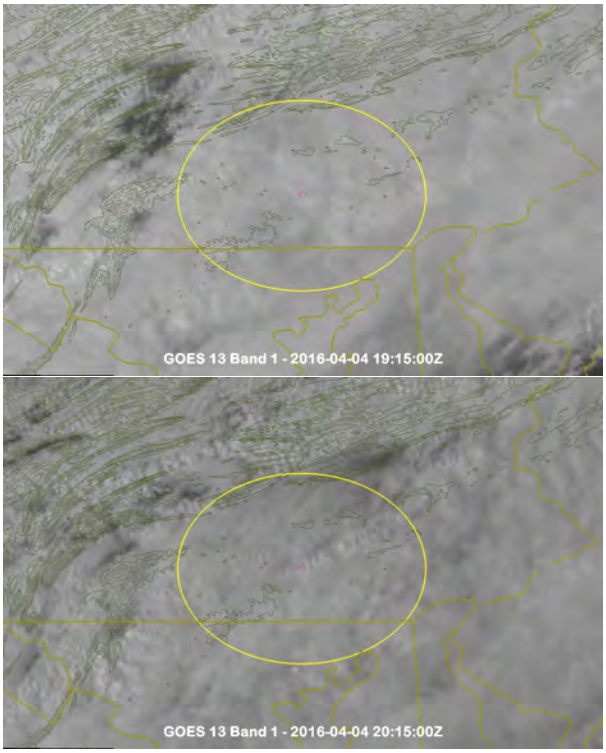

FIG. 5: GOES 13 visible imagery at (top) 1915 UTC and (bottom) 2015 UTC 04 April 2016. Topography is contoured in gold.

2.1 *Radar Imagery*

While the visible satellite imagery can reveal a decrease in the total column cloud amount, it does not show the heights at which this is occuring. This can be seen in the DOW scans if a feature can be correlated with one in the satellite. The left panel of Fig. 6 overlays the 2° PPI scan corresponding with a visible satellite image. Not only is the area of thinner cloud marked by a distinct lack of returns on the radar, but there is a line of increased reflectivities along the leading edge corresponding to the thin cloud line seen in satellite. Therefore, this drier air can be tracked by radar and a number of the airmass's

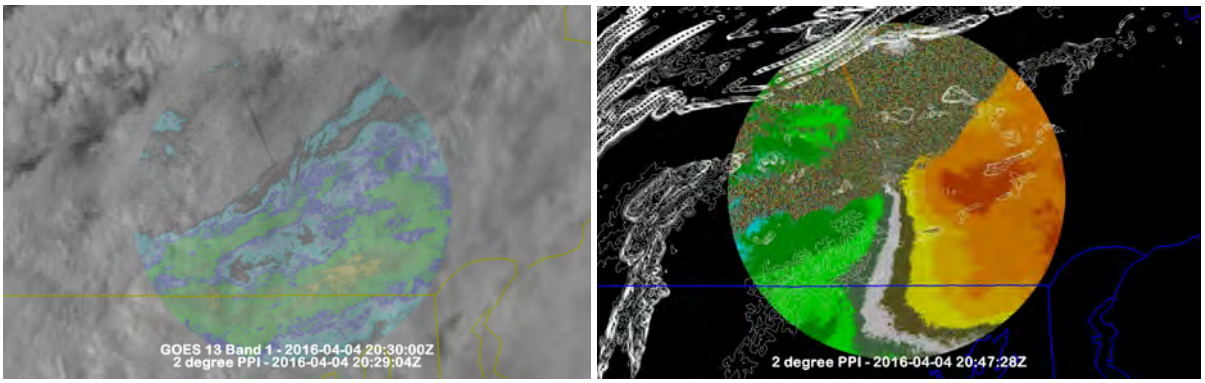

FIG. 6: (Left) 2° PPI of reflectivity at 2029 UTC and GOES 13 visible imagery at 2030 UTC 04 April 2016. (Right) 2° PPI of radial velocity at 2047 UTC 04 April 2016.

properties could be calculated, such as its propagation speed by comparing multiple time periods (Fig. 6).

Another feature that can be observed in the radar is the descending air's vertical structure. Figure 7 shows an RHI scan when this airmass is just upstream of the radar's location. The depth is higher at the leading edge than immediately behind. This structure is characteristic of a gravity current and has been observed in other remote sensors when cooler air enters a valley, especially when an inversion is initially in place. To put this observing into more context requires the use of numerical simulations.

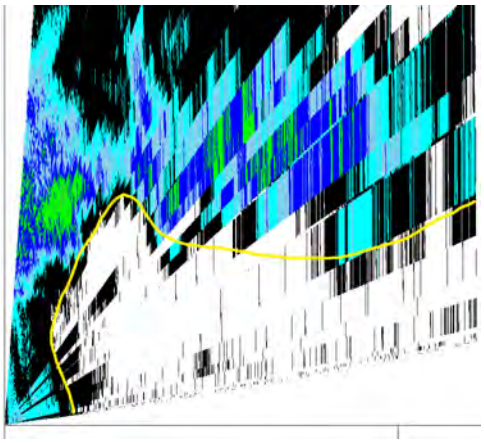

FIG. 7: 233° RHI scan of relfectivity at 2046 UTC 04 April 2016.

2.2 *WRF Simulation*

A simple model setup used the WRF-EMS system to place a 4-km domain covering Pennsylvania within the analysis fields from the 12-km NCEP NAM simulation for the IOP 2 time period. The simulations were run using a laptop with eight Intel i7 processors and the four hour runtime was completed in 16 minutes. Simple evaluations can be made by examing the 850 mb relative humidity field (Fig. 8). While lagged by 1-2 hours, there is an area of lower values to the lee that propagates from west to east, as observed in the satellite imagery.

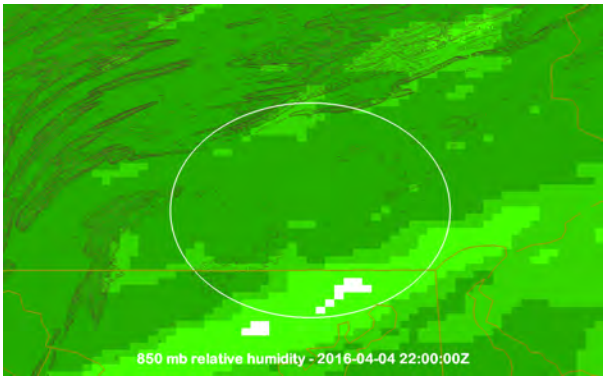

FIG. 8: 850 mb WRF relative humidities at 2200 UTC 04 April 2016.

Figure 9 shows a N-S vertical cross-section of the merdional wind speed over the Appalachians. The higher values occur with the low-level postfrontal northerlies. As the leading edge of this layer reaches the mountain crest, its vertical depth increases and remains so until descent to the flatter ground on the leeside is complete. This is additional evidence that the DOW data shows a gravity current intrusion.

3. MEDOW IOP 3 - SQUALL LINE

While the desired precipitation event had occurred during IOP 2, the forecast for the final day of the deployment called for thunderstorm activity. The convection was tied to an occluding cold front passing by the study area on the morning of 07 April (Fig. 10). The DOW was deployed and began taking observations a few hours prior to the passage of this front.

Besides the front, the Appalachians also had a large influence on the propoagation of the storms. Radar loops (such as `www2.mmm.ucar.edu/imagearchive`) show a line

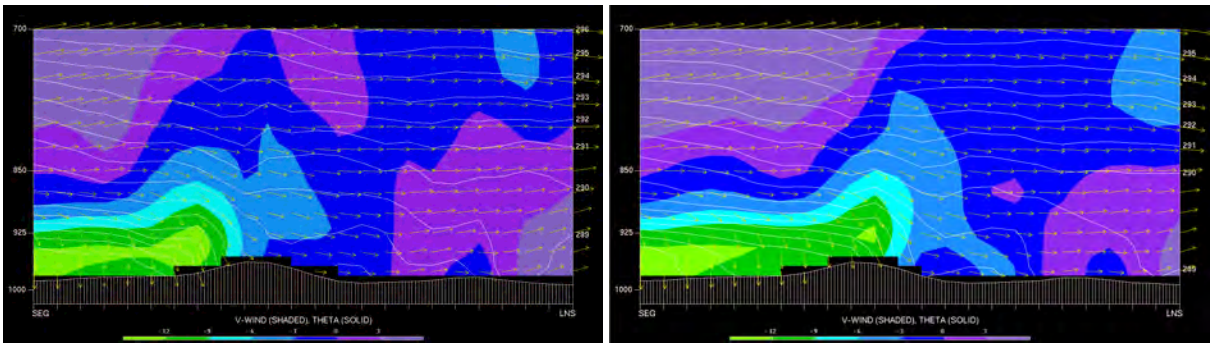

FIG. 9: Vertical cross-section of WRF meridional wind speeds at 2015 (left) and 2030 (right) 04 April 2016.

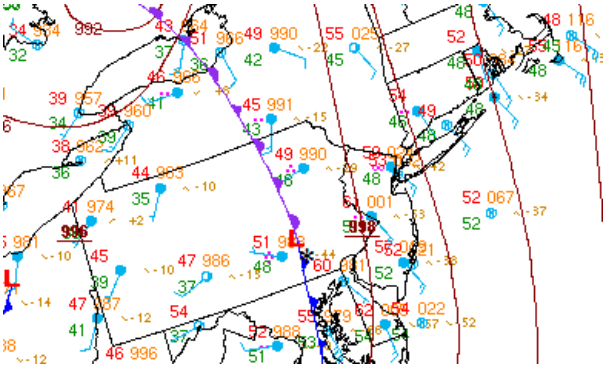

FIG. 10: WPC surface analysis for 18 UTC 07 April 2016. Millersville is shown by the asterisk.

of eastward moving cells as far north as Tennessee. However, the northern edge of this line dissipated upon reaching the mountains and only the portion that passed around the southern end of the mountains would remain intact. After reaching the leeside, discrete lines would continue to build to the north of the original squall line. Many of these segments develop bows over some portion of their length. The DOW site experienced strong wings and small hail, and further east in the same county the wind speeds would become significant enough to uproot trees and damage scoreboards as shown in Figure 11.

3.1 *Radar Imagery*

The bowing segment crossing southeast Pennsylvania first formed north of the DC area in northern Maryland. Ironically, given the use of the DOW to fill a radar hole, this area is at the edge of both the DOW and WSR-88D in Sterling, VA. However, radar features closer to the DOW location suggest a possible mechanism for the bow echo initiation in this area.

Figure 12 shows radial velocity PPI's depicting two different boundaries. Comparing with surface stations show that the trailing boundary is the primary occluding front. The other boundary is still under investigation. Over this time period, the front has almost reached the leading boundary at the latitude of the DOW and, based on the relative orientations, has possibly already reached further to the south where a bowing segment can first be seen. Since weak storm cells are present along this line, a bow echo could be initiated by the squall line - cell merger mechanism described by Burke and Schultz (2004).

FIG. 11: Storm damage on 07 April 2016 within the Octorara School District (LancasterOnline).

An important analogue to this event appears to be the serial derecho of 15-16 November 1989. Surface analyses depicted a squall line initially extending from the Gulf of Mexico north to Lake Erie, but it would only be the portion from Alabama southward that would continue eastward after the rest encountered the Appalachians. This segment would trigger a F4 tornado at Huntsville, and more analyzed squall lines would be placed to the north of this feature after it passed to the leeside. A new squall line would eventually build north up to and beyond Pennsylvania. This agrees well with the evolution of the bow echoes observed during the MEDOW event.

4. SEAR-MAR RF02/03 - COLD FRONT

The primary scientific objective stated in the SEAR-MAR project proposal was to obtain observations of the small-scale structure of a cold front during its passage over

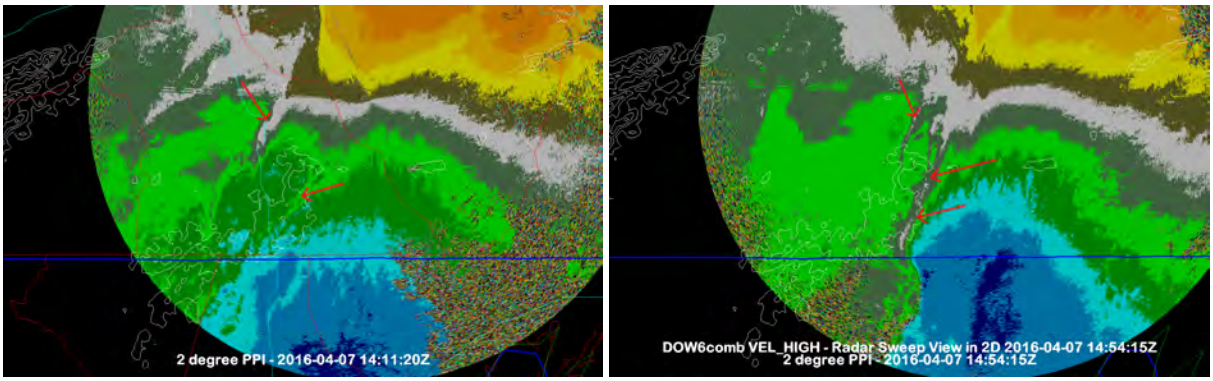

FIG. 12: PPI of radial velocity at 1411 and 1454 UTC 7 April 2016.

the Appalachian mountains. To acheive this goal, the Millersville PI's created a flight plan consisting of relatively short cross-front legs that would be displaced southward after each pass. The location of the legs could be shifted along a line running from the windward to the leeward side of the mountains in order to observe the front prior to and during its interaction with topography.

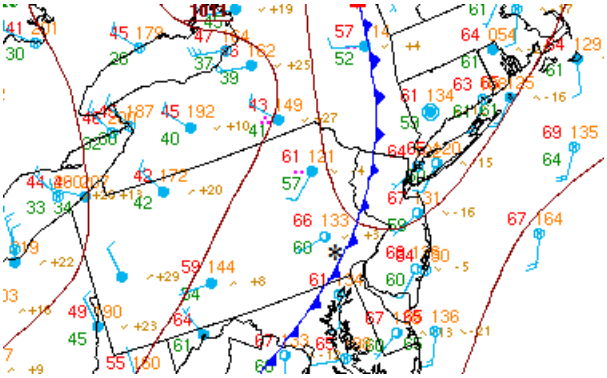

FIG. 13: WPC surface analysis for 18 UTC 06 November 2017. Millersville is shown by the asterisk.

The first and only cold front this track would be applied to crossed the study area on 6 November 2017. The WPC surface analysis places the front west of the mountains at 15 UTC along a SW-WNW wind shift and 10°F temperature drop. By 18 UTC (Fig. 13) and 21 UTC, the front was being analyzed to the east of the study area due to a shift in the winds to the WNW. However, the largest temperature gradient was still directed west of the study area and there was a second wind shift from WNW to NNW. Figure 14 shows the ASOS observations for Lancaster airport. While there is a clear wind shift between 14-17 UTC, the second shift between 20-23 UTC is the one associated with the temperature drop and the main front. These features can also be seen in the flight-level winds for the two King Air flights which occurred that day, one in the morning and one in the afternoon.

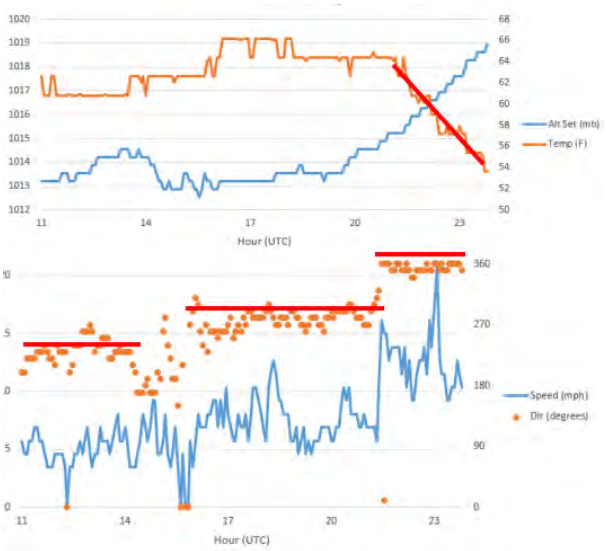

FIG. 14: Temperature and altimeter setting (top) and wind speed and direction (bottom) at KLNS from 11-24 UTC 6 November 2017. Wind shifts and strong temperature falls are annotated in red.

4.1 *Flight-level Winds and Temperatures*

Figure 15 shows a portion of the morning King Air flight track from 1440-1529 UTC. As the aircraft approached the NW corner of its pattern, winds were from the WSW and temperatures were near 8-9°C. At the end of this leg and during the next front-parallel segment, the winds had shifted to the WNW and temperatures had fallen to less than 5°C indicating the post-frontal airmass had been reached. On the returning cross-front leg, and through the rest of the morning flight, winds would remain from the WNW, leading to an assumption that the front had passed by the study area. On the other hand, while the winds remained constant on the return leg, temperatures increased back to pre-frontal values of 8-9°C (Fig. 15), suggesting that a second wind shift has developed ahead of the airmass boundary.

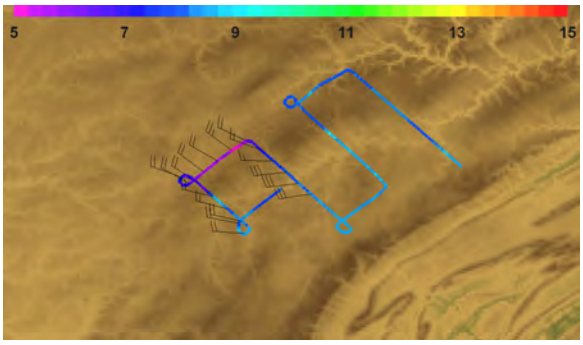

FIG. 15: King Air flight-level winds and temperatures from 1440-1529 UTC 6 November 2017.

Over five hours later, the afternoon flight along the lee of the mountains revealed no winds with the southward component earlier seen ahead of the front (Fig. 16). However, the last two along-front legs showed the same temperature fall that was previously observed while on the upwind side of the mountain range. Furthermore, some of the winds on the back leg had started to shift to an even more northly direction. This suggests that the afternoon flight was able to cross the frontal zone as well. A more detailed comparison of the front's properties while upstream and downstream of the topography will still be possible.

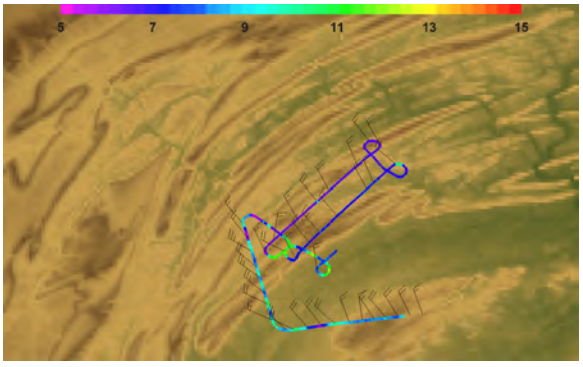

FIG. 16: King Air flight-level winds and temperatures from 2055-2135 UTC 6 November 2017.

Another interesting feature of this flight is seen in the ascending leg for the return ferry. The temperatures would flucuate by $\approx 2^{\circ}$C in a periodic manner. Given the front's movement past the terrain by this time, these would appear to be gravity waves forming in the post-frontal air. This phenomenon was another one of the propsoed research foci for the project, and a separate IOP dedicated to this will be described further in the next section.

4.2 *WRF Simulation*

To gain a broader view of the features which may have been present during the IOP, another WRF simulation was performed with the same setup as used in the MEDOW IOP 2 event. During the morning period, the temperature and wind field at the flight level contain prominent wind shifts in close proximity to the largest changes in temperature (not shown), as seen in the first flight. Two hours later at 17 UTC, the wind shift to the north of the E-W portion of the mountain range has moved rapidly eastward in conjunction with its associated temperature gradient (Fig. 17). Further to the south, the wind shift has also moved further east to over Millersville. However, the largest drop in temperaturs is still located on the upwind side of the Appalachians, again in agreement with the King Air observations.

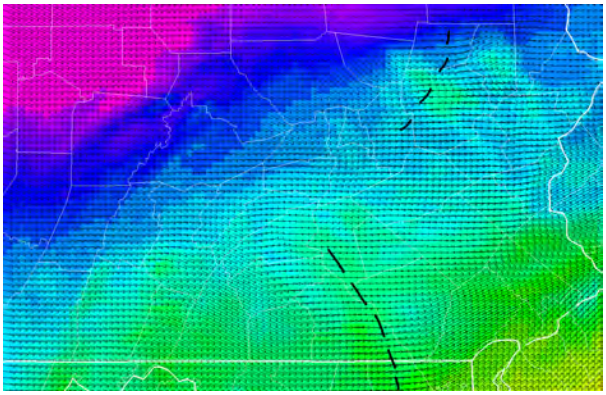

FIG. 17: WRF wind vectors and temperatures (color-shaded every 2°C) at 600 mb.

A front of this nature with the temperature decrease not coincident with the strongest pressure trough or wind shift is not unknown in the field of meteorology. Schultz (2005) reviewed ten different formation mechanisms for the prefrontal trough. The one most likley relevant to this case is due to interaction with a lee trough, although there are six internal mechanisms and frontal dynamics were a major focus of the initial deployment proposal.

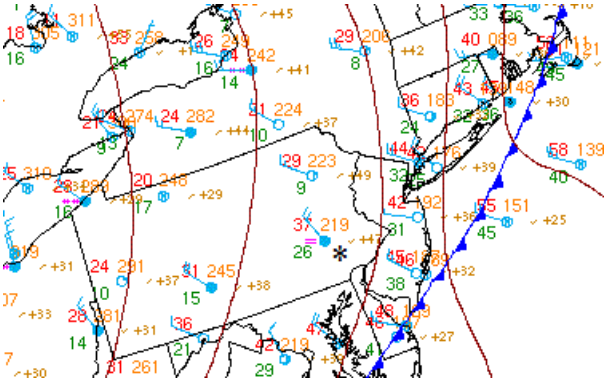

FIG. 18: WPC surface analysis for 12 UTC 10 November 2017. Millersville is shown by the asterisk.

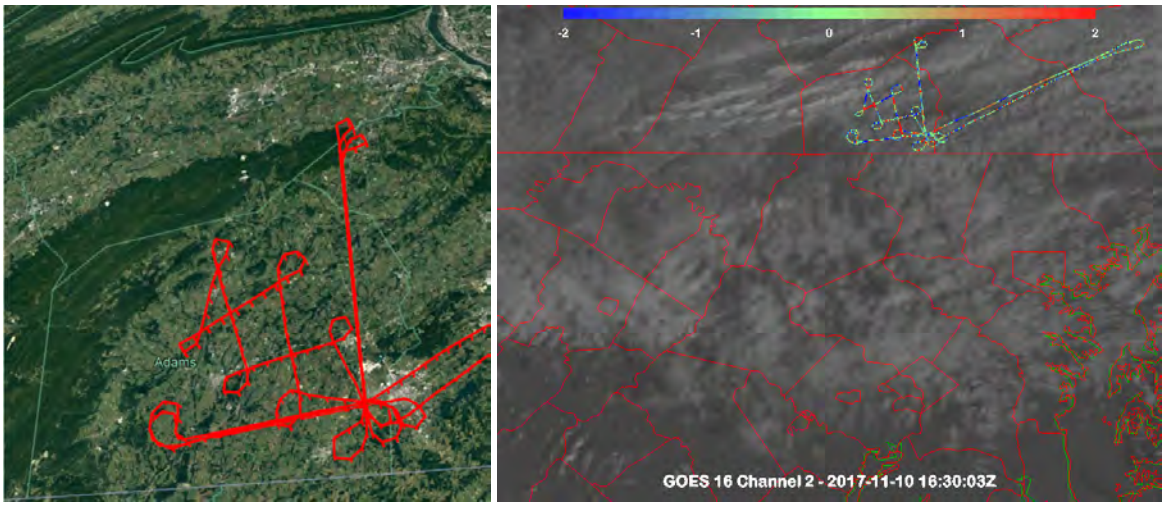

FIG. 19: Flight track overlaid on Google Earth imagery (left). Flight track of vertical velocity overlaid on GOES 16 visible imagery at 1630 UTC 10 November 2017 (right).

5. SEAR-MAR RF07 - Postfrontal Waves

The last ridgeline encountered by an airmass crossing the Appalachians is the Blue Ridge mountains. This range is already well known in mountain wave research due to the famous study by Smith (1977) using aircraft observations to evaluate linear theory predictions. The northern end of of the Blue Ridges is located WNW of Millersville, and it is at this point that the Appalachians make a 50° turn to the right. Winds nearly from the west produce mainly N-S oriented wave clouds, while winds with a primarly northern component produce cloud trains oriented in a more E-W direction. An airflow from the more intermediate northwestern direction should produce both types of waves which may interact in unique, and mostly unobserved, ways. These northwest, post-frontal winds occurred during the morning of 10 November 2017 (Fig. 18).

The flight plan designed to study these interactions including stacked legs oriented normally to both of the forcing ridgelines (Fig. 19). Between these, a series of zigzagging ascending and then descending legs were placed in an attempt to intersect both sets of wave trains. The lowest pair of legs were originally at 1750' and 3250' AGL, but during the actual flight it was found that the boundary layer extended to both of these levels. For this reason, an additional higher leg was added at 7750' AGL, and the second pair of zigzagging tracks was made at a constant 6250'.

As the day progressed, conditions were increasingly unstable, and many clouds were of a more cumuliform character, especially along the eastern portion of the flight track (Fig. 19). However, close to the mountains, trains of wave clouds were visible. To the south, the clouds were oriented in a N-S direction. Further north, the orientation is more E-W, though there are breaks in the cloud bands suggesting the effect of the mountain waves from the first ridgeline. While the north end of the N-S stacks and the last of the intermediate legs crossed into this portion of the visible imagery, most of the flight track was located in regions with the orientation of the first set of wave clouds.

While it is not apparent in the cloud field, the in-flight vertical velocities do suggest the possibility of two sets of waves along the E-W stacked legs. Performing a Fourier analysis of the leg at 6250' was assigned as homework to Millersville's Statistics for the Integrated Sciences class. Resulting power spectrums (Fig. 20) show the dominant peak in the second harmonic (≈8-10 km), but a second peak occurs in the tenth harmonic. Reconstructions using just these two wavelengths agree reasonably well with the actual vertical velocities (Fig. 20). More detailed analysis of this case has not been done, though the observations themselves were described by Keebler (2018).

Acknowledgments: The author would like to thank Alycia Gilliland of the Center for Severe Weather Research and Dave Plummer, Larry Oolman, and Tom Drew of the University of Wyoming for brining all this instrumentation to Millersville and for their extraordinary patience and flexibility in working with the faculty and achieving results such as these. The author acknowledges the extremely beneficial Educational Deployment program funded by the National Science Foundation and coordinated by the Earth Observing Laboratory.

References

Billings, B. J., S. A. Cohn, R. J. Kubesh, and W. O. J. Brown, 2018: An educational deployment of the Mobile Integrated Sounding System. *Bull. Amer. Meteor. Soc.,* In press.

Burke, P. C., and D. M. Schultz, 2004: A 4-yr climatology of cold-season bow echoes over the continental United States. *Wea. Forecasting,* **19,** 1061–1074.

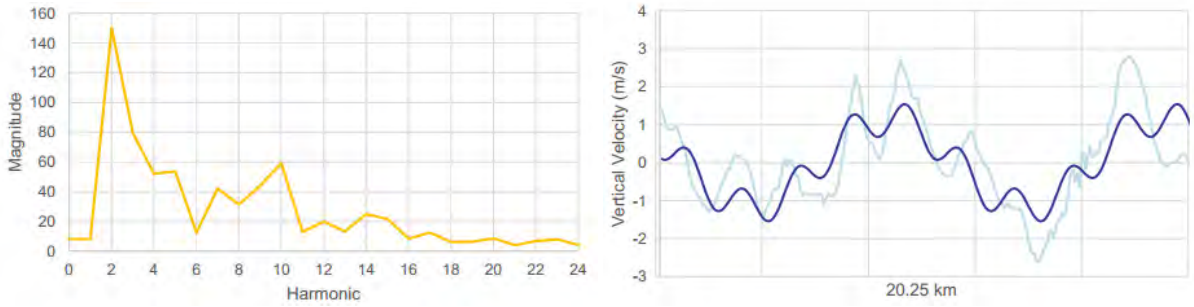

FIG. 20: Power spectrum of vertical velocities from 1439-1443 UTC 10 November 2017 (left). King air vertical velocities (cyan) and reconstruction from harmonics 2 and 10 (dark blue) for same flight leg (right).

Keebler, T. B., 2018: Gravity waves observed during the SEAR-MAR UW King Air deployment. *43rd Northeastern Storms Conference,* Saratoga Springs, NY

Milrad, S. M. and C. G. Herbster, 2017: Mobile radar as an undergraduate education and research tool: The ERAU C-BREESE field experience with the Doppler on Wheels. *Bull. Amer. Meteor. Soc.,* **98,** 1931–1948.

Schultz, D. M., 2005: A review of cold fronts with prefrontal troughs and wind shifts. *Mon. Wea. Rev,* **133,** 2449–2472.

Smith, R. B., 1976: The generation of lee waves by the Blue Ridge. *J. Atmos. Sci.,* **33,** 507–519.